13th International Conference on
Structural Health Monitoring of Intelligent Infrastructure
DOI: 10.3217/978-3-99161-057-1-041

Reliability Assessment of Structural Health Monitoring Systems using Model – Assisted Probability of Detection and Bayesian Model Updating

Yogi Jaelani[1], Francesca Marsili[1], Jan Grashorn[1], Sven Knoth[2], Sylvia Keßler[1]
[1]Engineering Materials and Building Preservation, Faculty for Mechanical and Civil Engineering, Helmut Schmidt University/University of the Federal Armed Forces Hamburg, Holstenhofweg 85, 22043 Hamburg, Germany
[2]Department of Mathematic and Statistics, Faculty of Economics and Social Sciences, Helmut Schmidt University/University of the Federal Armed Forces Hamburg, Holstenhofweg 85, 22043 Hamburg, Germany
email: yogi.jaelani@hsu-hh.de

ABSTRACT: Structural health monitoring (SHM) is a key method for assessing the condition of civil infrastructure, detecting and localizing damage through continuous data acquisition. Damage detection methods are divided into physically based approaches, using finite element (FE) models, and data-driven approaches, relying on signal processing. A key challenge in SHM is the lack of data from the damaged state, which complicates the validation of the technique. However, the successful deployment of SHM systems on real civil infrastructure depends mainly on their reliability. For non-destructive testing (NDT) systems, the Probability of Detection (POD) is an accepted approach for quantifying reliability. In contrast to NDT, there is no generally applicable procedure to assess the reliability of SHM systems.
This study addresses this gap by evaluating SHM reliability with POD models and data generated from calibrated FE models. These FE models are calibrated through Bayesian inverse methods. To manage computational challenges, generalized Polynomial Chaos Expansion (gPCE) surrogate models are employed. These methods are tested using vibration-based measurements on a laboratory-scale four-degree-of-freedom (4-DOF) wood frame. The results highlight the use of MAPOD and limitations of the method, emphasizing their potential to enhance SHM reliability and enable smarter infrastructure systems.

KEY WORDS: MAPOD; SHM; Bayesian inverse methods; vibration-based measurements.

1 INTRODUCTION

Structural Health Monitoring (SHM) is a key method for assessing the condition and integrity of civil infrastructure through continuous or periodic data acquisition. By deploying sensor networks, SHM systems are capable of detecting and localizing damage of structures, thereby enhancing maintenance strategies and extending service life. Damage detection methods in SHM are typically categorized into two major classes: physics-based methods, which utilize for example finite element (FE) models to simulate structural behavior; and data-driven methods, which rely on signal processing, statistical analysis, and machine learning [1].

A major challenge in SHM is the lack of damaged-state data, which complicates the validation and benchmarking of diagnostic techniques. This issue becomes critical when aiming to ensure the operational reliability of SHM systems in real civil infrastructure applications. While Non-Destructive Testing (NDT) technologies benefit from standardized reliability assessment procedures such as the Probability of Detection (POD), the SHM community is still developing a generally applicable methodology for quantifying SHM system reliability.

POD is a metric used to evaluate the performance of Inspection system of NDE. POD quantifies the likelihood that a flaw of a given size will be reliably detected by the inspection system NDE. POD curves have been widely applied in the aerospace and nuclear power industries to ensure structural safety [2–4]. The conventional approach for estimating POD curves as used in the aerospace industry is based on empirical testing as outlined in MIL-HDBK-1823A [2]. This approach requires the generation of a sufficiently large and representative data set covering a range of flaw sizes. Two primary techniques are commonly used: the **Hit/Miss** method and the **â vs. a** (response vs. flaw size) method. These procedures form the foundation of standardized POD analysis in NDE.

In contrast, the Model-Assisted Probability of Detection (MAPOD) approach integrates physics-based model simulation for estimating POD. MAPOD aims to extend and complement the basic MIL-HDBK methodology by reducing (though not eliminating) the need for physical testing samples.

The application of MAPOD has been investigated in several studies [7–9]. Smith et al. [8] successfully conducted a fully model-assisted POD validation for immersion ultrasonic inspection targeting embedded flat-bottom holes. Their results demonstrated equivalence to those obtained using the conventional MIL-HDBK-1823 approach.

Knopp et al. [7] explored a MAPOD approach for evaluating crack detection in a two-layer airframe structure with countersunk fasteners using Eddy Current Testing (ECT). The study involved 171 fasteners, including 38 with known cracks, with crack lengths ranging from 0.69 mm to 4.29 mm. Physical models were calibrated with experimental data, and 5000 synthetic data points were generated via Monte Carlo simulation for MAPOD estimation. The results showed excellent qualitative agreement between the empirical and simulation-based POD curves, although uncertainties in the input parameters were not explicitly addressed.

By leveraging FE models or numerical simulations, MAPOD can significantly lower the time, cost, and logistical complexity of traditional POD studies [7]. This numerical simulation-based method has great potential in evaluating the reliability of SHM systems, where empirical data is often limited or difficult to obtain.

This study proposes a framework for evaluating the reliability of SHM systems using POD and MAPOD models. The framework is enhanced by simulated data generated from

DOI: 10.3217/978-3-99161-057-1-041

finite element (FE) models, which are calibrated in the reference/undamaged state using Bayesian inverse methods to capture uncertainties and improve prediction accuracy based on experimental observations. As a result, simulations of parametric variations, such as the initiation and progression of damage, can be conducted with higher accuracy, thereby improving the predictive capability and overall reliability of the SHM system.

To address the computational demands of FE simulations, surrogate models based on generalized Polynomial Chaos Expansion (gPCE) theory are employed.

The calibration of the FE model is performed by applying a Polynomial Chaos Expansion-based Kalman Filter (PCE-KF). This method is validated using a laboratory-scale experiment involving a four-degree-of-freedom (4-DOF) wooden frame subjected to vibration-based measurements. The measurements are performed under both reference and changed states, where the changes are introduced through controlled mass variations.

The results demonstrate the feasibility of applying MAPOD techniques within the SHM context and provide insight into the limitations and practical considerations of this approach. Ultimately, this work contributes to the development of reliable SHM systems for civil infrastructure.

2 METHODOLOGY

The overall workflow proposed for the MAPOD construction is illustrated in Figure 1, while a detailed explanation of each component is provided in the subsequent sections.

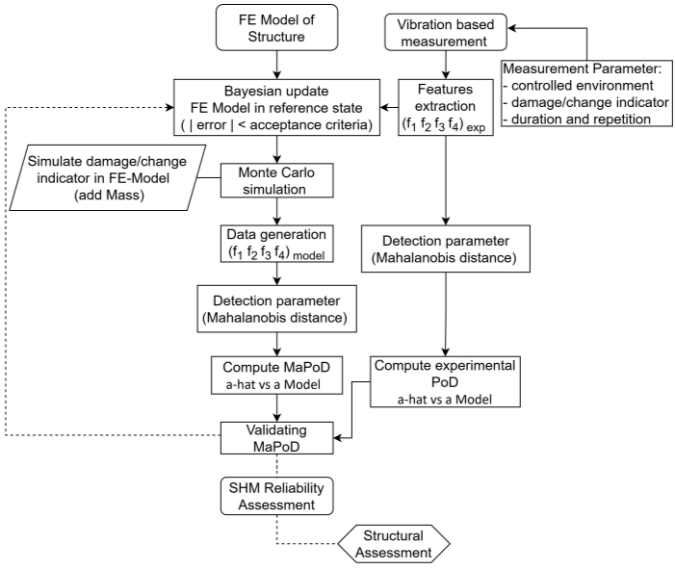

Figure 1. MAPOD model building process

2.1 Experimental Setup

A laboratory-scale four-story wooden frame structure is designed to simulate the response of four degrees of freedom system. To achieve this, the column dimensions are carefully adjusted to ensure that the stiffness in one translational direction is significantly greater than in other translational or rotational directions. The column cross-section is 300 mm by 6.4 mm. The total height of the wooden frame is 1000 mm, with a width of 500 mm. Each story has a height of 250 mm. The beam cross-section is 60 mm by 60 mm. The columns are constructed from laminated wood sheets, while the beams are made of solid wood. The mass of each structural element is determined by weighing the components prior to assembly. The frame is instrumented with triaxial accelerometers to record its vibration response under random excitation induced by a handheld rubber hammer. A data acquisition system from Dewesoft and MMF KS903B100 triaxial accelerometers are used in this experiment. The experimental setup is illustrated in Figure 2, and the structural geometry and mass is summarized in Table 1.

Table 1. Structural geometry and mass

Geometry [mm]		Mass [gr]	
Column cross-section	300x6.4	Column 1 Column 2	885 915
H, Height	1000	Beam 1st Floor	1122
		Beam 2nd Floor	1060
Beam cross-section	60x60	Beam 3rd Floor	1046
L, Length	500	Beam 4th Floor	1020
		Triaxial Accelerometer	11

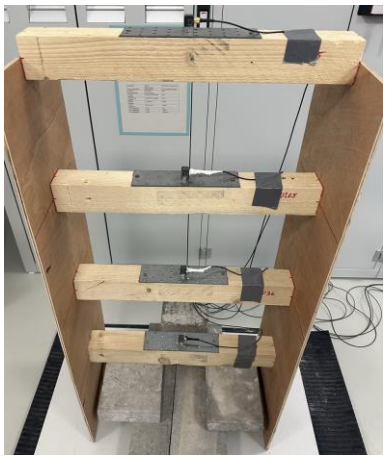

Figure 2. Experimental setup

The measurements are conducted under both reference (undamaged) and changed (damaged) states**.** The changed state is simulated by incrementally adding mass to the fourth floor of the structure. For each state, vibration responses are recorded for 90 seconds at a sampling rate of 1000Hz, with each test repeated at least 15 times to ensure statistical consistency. The experiments are performed over several days, from March 24th to March 29th 2025, to ensure sufficient data collection and to capture a broader range of variability even under stable environmental conditions.

All experiments are conducted under constant room temperature ranges and humidity conditions. This experimental setup serves as the basis for validating the MAPOD analysis compared to real physical test data. Details of the measurement set and repetition are provided in Table 2.

DOI: 10.3217/978-3-99161-057-1-041

Table 2. Measurement set

Measurement Set	Added Mass [gr]	[%] to the Mass of 4th floor	Repetition
Reference	0	0	267
Mass 1	25	2,4 %	69
Mass 2	51	4.9 %	55
Mass 3	75	7.3 %	20
Mass 4	102	9.9 %	70
Mass 5	153	14.8 %	66
Mass 6	204	19.8 %	55
Mass 7	255	24.7%	15

2.2 Finite element model and Bayesian updating

A three-dimensional finite element (FE) model of the four-story wooden frame structure is developed in Ansys to simulate its modal dynamic response. The model geometry reflects the actual dimensions of the physical structure, incorporating column and beam cross-section. Shell elements are used to represent the thin column sections, while beam elements are used to represent beams. The beam-column connections are assumed to be rigid. The boundary conditions simulate fixed line support at the base, consistent with the physical setup.

Material properties are initially assigned based on measured values. The material density is then calculated as the ratio of mass to volume for each element. The elastic modulus is unknown and is treated as random variable in wood properties. In addition to the elastic modulus, the thickness of the columns is also modeled as a random variable, accounting for imperfections in the thickness of the wood elements. The elastic modulus and column thickness are then treated as input random parameters in the Bayesian model updating. Meanwhile the natural frequencies and mode shapes obtained from modal analysis are used as output (observed) parameters for the Bayesian model updating.

2.3 Polynomial Chaos Expansion based Kalman Filter

A Bayesian model updating approach is applied to minimize discrepancies between the outputs of the FE model and the experimental measurements. The uncertain parameters, such elastic modulus and thickness of columns, are treated as random input parameters $\boldsymbol{Q} \in \mathbb{R}^{N_n}$ where N_n is the number of input parameters, modeled as Gaussian independent variables

$$\boldsymbol{Q} = \mathcal{N}(\boldsymbol{\mu}_Q, \boldsymbol{C}_Q) \tag{1}$$

where $\boldsymbol{\mu}_Q \in \mathbb{R}^{N_n}$ is the vector of mean values and $\boldsymbol{C}_Q \in \mathbb{R}^{N_n \times N_n}$ is the covariance.

The system random inputs are transformed by a forward model operator $\mathcal{M}$ into the outputs $\boldsymbol{Y} = \mathcal{M}(\boldsymbol{Q}) \in \mathbb{R}^{N_m}$ where N_m is the number of measured outputs. The measurement $\boldsymbol{Z} \in \mathbb{R}^{N_m}$ is affected by an error $\boldsymbol{E} \in \mathbb{R}^{N_m}$, which follows a normal distribution and combines linearly with the measured output

$$\boldsymbol{Z} = \mathcal{M}(\boldsymbol{Q}) + \boldsymbol{E}, \boldsymbol{E} = \mathcal{N}(0, \boldsymbol{C}_E) \tag{2}$$

where $\boldsymbol{C}_E \in \mathbb{R}^{N_m \times N_m}$ is error covariance. The scope of the Bayesian updating is to improve the estimation of the random input $\boldsymbol{Q}$ given output measurements $\boldsymbol{z}$. An efficient approach to Bayesian updating consists in applying the linear Bayesian Filter

$$\boldsymbol{Q}' = \boldsymbol{Q} + \boldsymbol{K}(\boldsymbol{z} - \boldsymbol{Y}) \tag{3}$$

where $\boldsymbol{Q}$ are prior parameter estimates, $\boldsymbol{Q}'$ are the posterior, $\boldsymbol{z}$ are output measurements, $\boldsymbol{Y}$ are measured system outputs and $\boldsymbol{K}$ is the Kalman Gain

$$\boldsymbol{K} = \boldsymbol{C}_{\boldsymbol{QY}}(\boldsymbol{C}_{\boldsymbol{Y}} + \boldsymbol{C}_{\boldsymbol{E}})^{-1} \tag{4}$$

where $\boldsymbol{C}_{\boldsymbol{Y}}$ is the system outputs covariance, $\boldsymbol{C}_{\boldsymbol{E}}$ is the error covariance and $\boldsymbol{C}_{\boldsymbol{QY}}$ is the covariance between system inputs and outputs.

The application of the linear Bayesian filter requires to assess the above mentioned covariances. This process is not straightforward in the case of implicit and/or non-linear forward model operators. To speed up the uncertainty propagation process and the application of the linear Bayesian filter, it is possible to represent each random variable in polynomial chaos expansion (PCE) form

$$\begin{aligned} \widehat{\boldsymbol{Q}} &= \textstyle\sum_{\mathcal{J}} \widehat{\boldsymbol{q}}_{\boldsymbol{\alpha}} \boldsymbol{\Phi}_{\boldsymbol{q},\boldsymbol{\alpha}}, \quad \widehat{\boldsymbol{Y}} = \textstyle\sum_{\mathcal{J}} \widehat{\boldsymbol{y}}_{\boldsymbol{\alpha}} \boldsymbol{\Phi}_{\boldsymbol{y},\boldsymbol{\alpha}}, \\ \widehat{\boldsymbol{E}} &= \textstyle\sum_{\mathcal{J}} \widehat{\boldsymbol{e}}_{\boldsymbol{\alpha}} \boldsymbol{\Phi}_{\boldsymbol{e},\boldsymbol{\alpha}}, \quad \widehat{\boldsymbol{Z}} = \textstyle\sum_{\mathcal{J}} \widehat{\boldsymbol{z}}_{\boldsymbol{\alpha}} \boldsymbol{\Phi}_{\boldsymbol{z},\boldsymbol{\alpha}} \end{aligned} \tag{5}$$

where $\widehat{\boldsymbol{q}}_{\boldsymbol{\alpha}}, \widehat{\boldsymbol{y}}_{\boldsymbol{\alpha}}, \widehat{\boldsymbol{e}}_{\boldsymbol{\alpha}}, \widehat{\boldsymbol{z}}_{\boldsymbol{\alpha}}$ are coefficients, $\boldsymbol{\Phi}_{[\cdot],\boldsymbol{\alpha}}$ multi-variate orthogonal polynomials for the quantity $[\cdot]$, and $\mathcal{J}$ represents the set of multi-indices $\boldsymbol{\alpha}$ truncated to the polynomial order p. In this case, the linear Bayesian filter takes the following form

$$\widehat{\boldsymbol{Q}}' = \widehat{\boldsymbol{Q}} + \boldsymbol{K}(\widehat{\boldsymbol{z}} - \widehat{\boldsymbol{Y}}) \tag{6}$$

and the covariances required to calculate the Kalman Gain can be analytically computed by the expansion coefficients. Detailed information about the polynomial chaos expansion based Kalman filter (PCE-KF) can be found in Rosic et al. (2012) and Rosic et al. (2013).

2.4 POD estimation and reliability metrics

The POD curve in this study is estimated using the â vs. a approach. The â vs. a model POD is a technique used in NDT to quantify the capability of a detection system based on continuous damage indicators. Unlike hit/miss POD methods, which rely on binary detection outcomes, the â vs. a model POD utilizes a continuous detection metric â that reflects measurable differences in the system's response between undamaged and damaged states. This approach allows for an assessment of detection performance, particularly in systems where subtle changes in dynamic characteristics, such as natural frequencies or mode shapes, are used to infer damage. In vibration-based monitoring, such metrics are often derived from modal parameter shifts or other features sensitive to structural changes.

The â vs. a model involves fitting a linear function to the response feature, â, as a function of the parameter of interest a,

$$\widehat{\boldsymbol{a}} = \beta_0 + \beta_1 \boldsymbol{a} + \boldsymbol{\epsilon} \tag{7}$$

where β_0 and β_1 are parameters that are estimated by performing a fit to the data and ϵ is a noise term, $\epsilon \sim \mathcal{N}(0, \sigma^2)$. The noise term ϵ is assumed to follow a normal distribution. The aforementioned parameters β_0, β_1 and σ are estimated in

DOI: 10.3217/978-3-99161-057-1-041

the usual way by deploying ordinal least squares. We can ignore the more elaborated Tobit regression modeling from MIL-HDBK-1832A [2], because the observed â values (see below) are far away from their natural bounds.

When multiple response features are available, a representative scalar value is needed to consolidate the relevant information into a single damage-sensitive metric. To address this, the Mahalanobis distance (MD) is employed as a fault indication metric. The Mahalanobis distance is a multivariate measure that accounts for correlations between variables, providing a statistically normalized distance of an observation from a reference distribution. For an observation vector $\boldsymbol{x}_i$ (e.g., the measured eigenfrequencies of a structure at a specific time or condition), and a reference data set (e.g., the average eigenfrequencies in the undamaged state) characterized by mean vector $\boldsymbol{\mu}$ and covariance matrix $\boldsymbol{\Sigma}$, the Mahalanobis distance is defined as

$$D_M(\boldsymbol{x}_i) = \sqrt{(\boldsymbol{x}_i - \boldsymbol{\mu})\boldsymbol{\Sigma}^{-1}(\boldsymbol{x}_i - \boldsymbol{\mu})} \tag{8}$$

To determine the statistical decision threshold for damage detection, the confidence interval approach based on the Chi-squared distribution is employed. Since the Mahanlaobis distance D_M follows follows a Chi-squared distribution with degrees of freedom equal to the number of variables d, the decision threshold is defined as:

$$\boldsymbol{T} = \sqrt{\boldsymbol{\chi}^2_{\boldsymbol{1-\alpha,d}}} \tag{9}$$

Where $\boldsymbol{\chi}^2_{\boldsymbol{1-\alpha,d}}$ denotes the critical value from the Chi-squared distribution at a confidence level of $1-\alpha$, and d is the dimensionality of the feature. For example, at a 99.9% confidence level and $d = 3$, the threshold is $\chi^2_{0.999,3} = 16.27$, corresponding to a Mahalanobis distance threshold of $T = \sqrt{16.27} \approx 4.03$. This captures the upper 0.1% of the reference distribution and yields a very strict false alarm rate.

The Probability of Detection (POD) as a function of damage size a is expressed as:

$$\boldsymbol{POD(a)} = \boldsymbol{\Phi}\left(\frac{\boldsymbol{a} - \boldsymbol{\mu_a}}{\boldsymbol{\sigma_a}}\right) \tag{10}$$

Where $\Phi(\cdot)$ is the cumulative distribution function of the standard normal distribution, and μ_a and σ_a are suitable parameters controlling the shape of the POD curve. These parameters are derived from the linear regression model, with $\mu_a = (T - \beta_0)/\beta_1$ and $\sigma_a = \sigma/\beta_1$, where β_0, β_1 and σ are the model parameters. The threshold corresponding to a 90% detection probability, a90 with POD(a90) = 0.9, is then calculated as $a_{90} = \mu_a + 1.645 \cdot \sigma_a$. To account for the uncertainty in this threshold, the value $a_{90/95}$, representing the damage size for 90% POD with 95% confidence bounds, is computed using the Delta method referred to MIL-HDBK-1832A [2]. These performance metrics are used to assess and compare the detection capabilities of the SHM system. Following the same methodology, the Probability of Detection (POD) is also calculated using data generated from the calibrated finite element (FE) model.

3 ANALYSIS

3.1 Data Analysis/Operational Modal Analysis

The recorded vibration data are analysed using operational modal analysis (OMA) to identify the dynamic parameters of the wooden frame. OMA is chosen because it enables the extraction of modal parameters under ambient or operational conditions without requiring controlled excitation forces. Using Artemis Modal Pro 7.2 software, the OMA is performed, and the natural frequencies (f), damping ratios (ς), and mode shapes of the structure are estimated. Based on the analysis results, four resonance frequencies are identified, corresponding to the four translational modes of the wooden frame. Figure 3 illustrates the identified mode shapes of the wooden structure in the reference state.

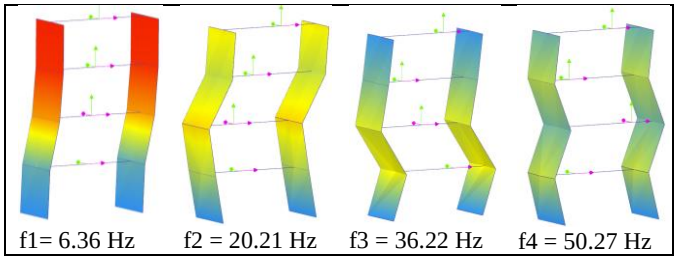

Figure 3. Mode shapes and frequency of wooden frame in reference state

OMA is also performed for all added mass configurations. Modal tracking is carried out to identify the mode similarities between each configuration to the reference state, with the Modal Assurance Criterion (MAC) threshold set to greater than 80%. The tracked resonance frequencies across all data sets are presented in Figure 4.

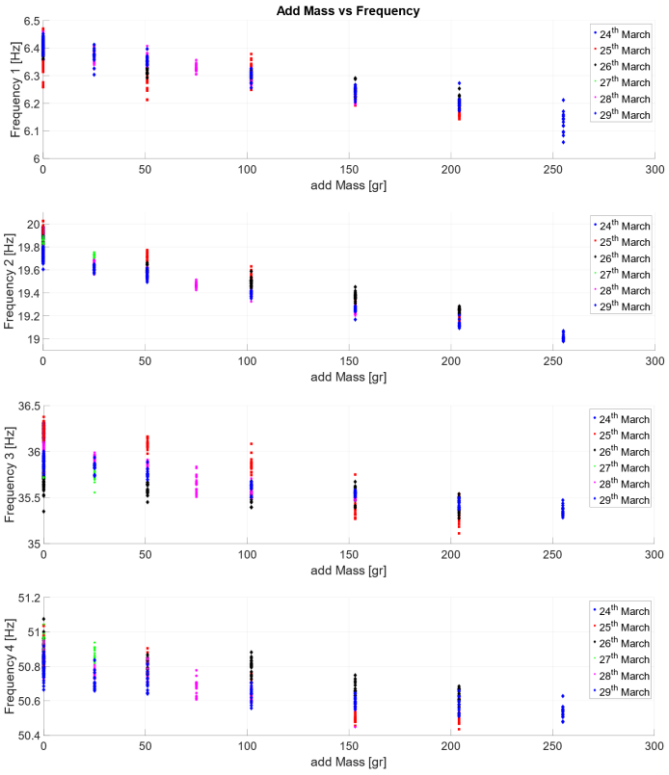

Figure 4. Tracked frequency (MAC > 80%) for the reference state and various added mass configurations

DOI: 10.3217/978-3-99161-057-1-041

From Figure 4, it can be observed that the addition of mass on the fourth floor affects the dynamic response of the structure, particularly the resonance frequencies. As the added mass increases, the natural frequencies tend to decrease, which is consistent with the theoretical expectation that an increase in mass leads to a reduction in the system's stiffness-to-mass ratio. In addition to the frequency shifts, the damping ratios of the structure were also examined; however, no clear trend was observed in relation to the parameter changes. Furthermore, the first four dominant mode shapes remained largely unchanged, indicating that the modifications had minimal influence on the modal characteristics.

The results of the Operational Modal Analysis in the reference state, as shown in Figure 3, are used as the baseline data for calibrating the FE-model through a Bayesian model updating approach. An overall Operational Modal Analysis, as shown in Figure 4, is used to compute the empirical Probability of detection.

3.2 Bayesian model updating

A finite element (FE) model of the structure is developed using Ansys Mechanical, based on the given structural conditions. The FE model is then calibrated through Bayesian updating to estimate random model parameters. In this study, two key parameters are considered: the elastic modulus of the columns and the column thickness, as previously described. The FE-Model in Ansys is illustrated in Figure 5.

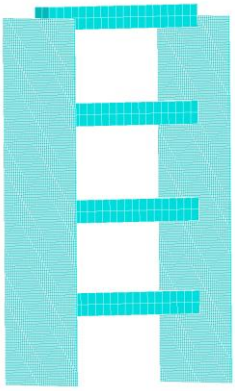

Figure 5. FE-Model in Ansys Mechanical

Initially, the prior distributions of the uncertain model parameters defined by their mean (μ) and standard deviation (σ) are established based on engineering judgment and available data. The Bayesian model updating is performed using the generalized Polynomial Chaos-based Kalman Filter (gPC-KF) approach. These methods incorporate measurement uncertainties to update the parameter distributions, resulting in posterior distributions (μ′, σ′) that reflect improved estimates conditioned on the observed vibration data. The summary statistics of both prior and posterior distributions are presented in Table 3 and the resulting posterior approximation distribution is shown in Figure 6.

The results of the Bayesian updating process show a reduction in the standard deviations of the posterior distributions, indicating improved parameter certainty in a model calibration. To assess the accuracy of the updated FE model, its predicted mean resonance frequencies – computed using the mean values of the parameters from the posterior distributions – are compared against those obtained from Operational Modal Analysis (OMA) in the reference state, as detailed in Section 3.1. The relative difference between the simulated and experimental frequencies observed for the four modes is 0.54%, which is well within the maximum relative error of 0.6% in reference data. This close agreement confirms the reliability of the Bayesian-updated model.

Table 3. Prior and posterior of random parameters

Parameter	Elastic Modulus of Column	Thickness of Column
Prior Mean value, standard deviation (μ, σ)	4000, 400 [MPa] σ = 0.1μ	6.4, 0.32 [mm] σ = 0.05μ
measurement error	0.6 %	
Posterior Mean value, standard deviation (μ', σ')	3800, 316 [MPa] σ' = 0.083μ'	6.18, 0.18 [mm] σ' = 0.29μ'
relative difference $\epsilon_i = \frac{\lvert f_{i\_FE\,model} - f_{i\_OMA} \rvert}{f_{i\_OMA}}$		0.54 %

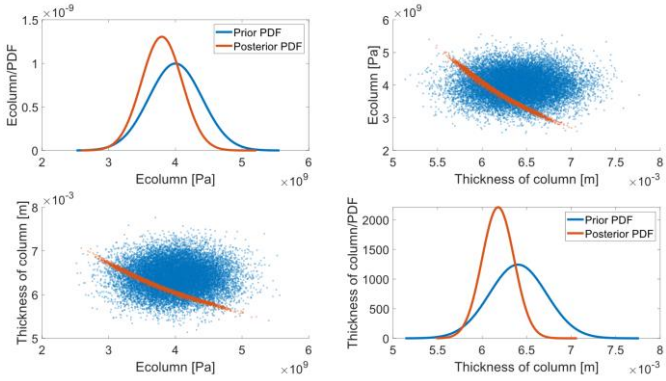

Figure 6. Results from updating with Bayesian model updating approach

Table 4. Comparison of resonance frequencies between the updated finite element (FE) model and experimental measurements from Operational Modal Analysis (OMA)

Mode No.	Frequency FE-Model	Frequency OMA	relative difference [%]	MAC [%]
1	6.39	6.40	0.21	97
2	19.91	19.81	0.53	90
3	36.16	35.97	0.54	90
4	50.81	50.56	0.10	98

Following the successful calibration of the FE model in the reference state, a Monte Carlo simulation is performed to generate modal frequency data for various added mass configurations. Based on the posterior distributions of the elastic modulus and column thickness, combined with discrete

DOI: 10.3217/978-3-99161-057-1-041

added mass values to simulate different structural states, 120 samples of frequencies are generated for each state. The additional masses varied from 0 to 200 grams in increments of 25 grams. The resulting dataset is then used as the input for computing the Model-Assisted Probability of Detection (MAPOD), providing a statistical basis for assessing the detection performance under varying conditions.

3.3 Simulation of Model-Assisted Probability of Detection

This section presents a comparative analysis between the experimental Probability of Detection (POD) and the Model-Assisted POD (MAPOD) derived from the simulations. The comparison aims to validate the simulation framework and assess its capability to replicate detection performance observed in physical experiments. The observed strategy is based on changes in modal frequencies associated with varying levels of added mass, simulating structural changes/damage.

Figure 7 illustrates the comparison of resonance frequencies identified from OMA experimental data measurements and those predicted by the calibrated FE model, demonstrating good agreement and confirming the effectiveness of the model updating process. Modes 1 and 2 are highly sensitive to the added mass, showing noticeable shifts in frequency. In contrast, Mode 3 exhibits only minor changes, while Mode 4 shows the least response to mass variation. This behavior is to be expected, as higher-order modes typically require more energy to be effectively excited and are thus less influenced by localized changes in structural mass [16,17]. Therefore, only Modes 1, 2, and 3 will be considered for further POD estimation, as they exhibit measurable sensitivity to the added mass and are thus more suitable for damage detection analysis.

To evaluate the consistency between the experimental POD and the MAPOD derived from simulated data, Mahalanobis distances from the 1st ,2nd and 3rd modes are computed and plotted against the corresponding flaw sizes, as shown in Figure 8. Finally, the POD curves are presented in Figure 9, comparing the empirical POD derived from experimental data with the MAPOD computed from the simulation results.

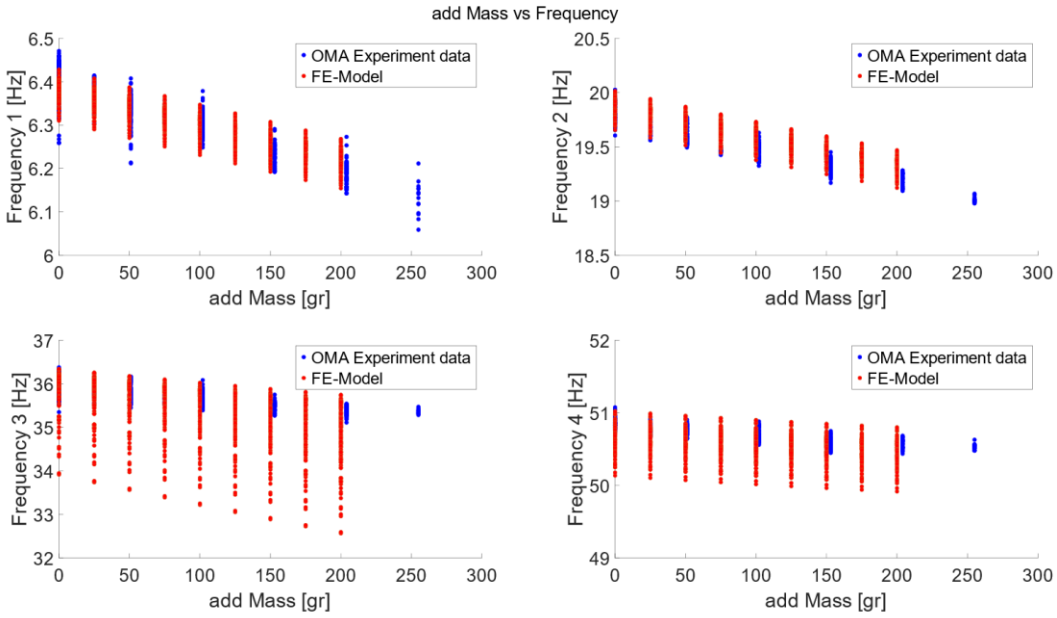

Figure 7. Added Mass-Frequencies comparison from OMA experimental data and FE-Model

DOI: 10.3217/978-3-99161-057-1-041

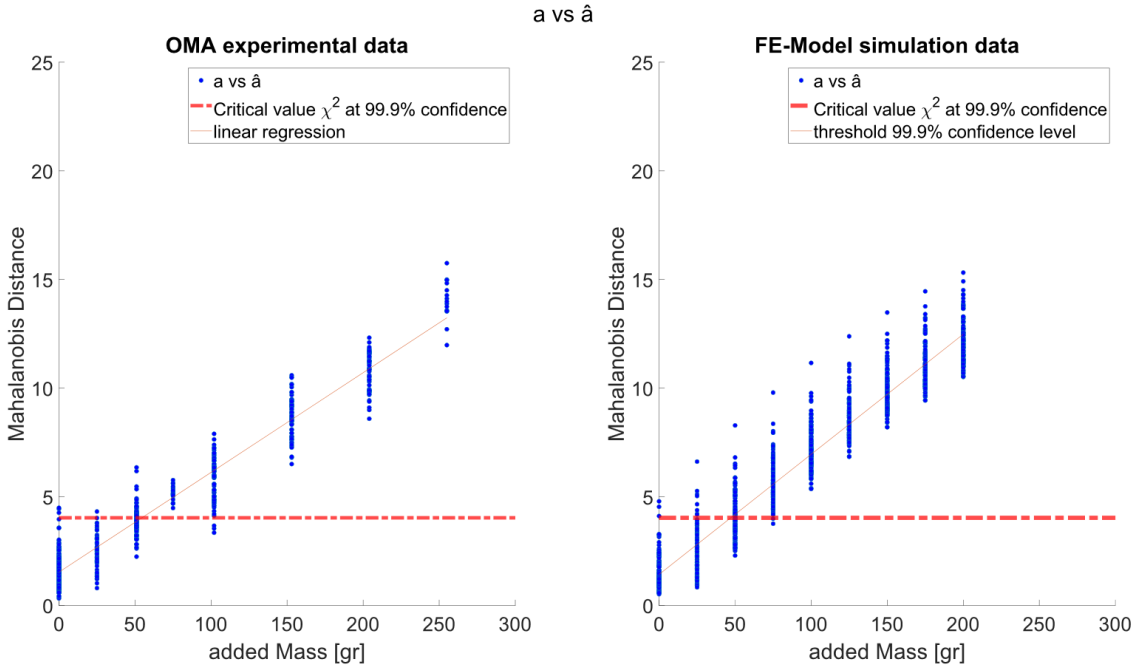

Figure 8. a vs â for OMA experimental data and FE-Model

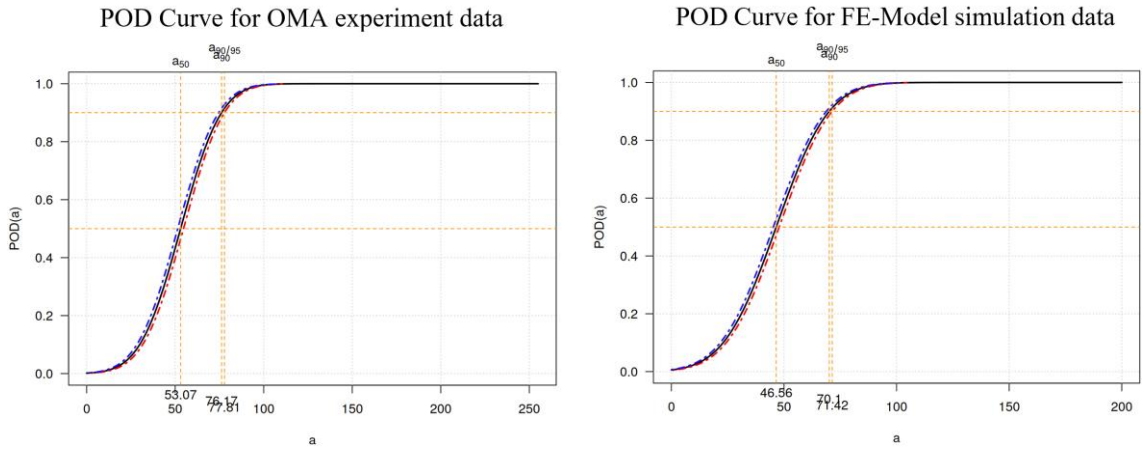

Figure 9. POD OMA experimental data and FE-Model simulation data

From Figure 9, the experimentally derived $a_{90/95}$ value from the POD curve is 77.81 grams, while the simulated MAPOD yields an $a_{90/95}$ of 71.42 grams, representing a relative difference of 8.2%. This $a_{90/95}$ value corresponds to 7,0% of the total mass of the fourth floor. These results indicate that the POD derived from the calibrated FE model in the reference state provides sufficient predictions of the structural response to varying added mass conditions on the fourth floor. The alignment between the experimental and simulated POD curves demonstrates that the simulation-based MAPOD can approximate the experimental detection, supporting its application for scalable and cost-effective SHM reliability assessments.

4 CONCLUSION AND OUTLOOK

This study presents a framework for evaluating the reliability of Structural Health Monitoring (SHM) systems using Probability of Detection (POD) and Model-Assisted POD (MAPOD) approaches. A laboratory-scale 4-DOF wooden frame structure was used as a case study, with varying mass configurations to simulate structural changes. Experimental modal data were collected using Operational Modal Analysis (OMA) and used to calibrate a Finite Element (FE) model through Bayesian updating. The updated FE-Model served as the basis for generating simulated response/modal data through Monte Carlo simulations under various mass configurations, enabling the construction of MAPOD curves.

The comparison between experimental POD and MAPOD simulation data shows the relative difference with less than 10% deviation in key detection metrics such as a $a_{90/95}$. The MAPOD approach can effectively supplement physical testing by providing scalable, repeatable reliability assessments with reduced experimental effort.

Outlook:

Future research should aim to extend the MAPOD framework by incorporating more complex damage scenarios—such as sequential cracking or cross-sectional area reduction leading to structural stiffness degradation—exploring a wider range of

DOI: 10.3217/978-3-99161-057-1-041

SHM sensing techniques and expanding the set of observed response features beyond the four considered in this study. Furthermore, integrating environmental and operational variability into the model could further enhance its predictive robustness. Finally, applying this method to real-scale structures will be a crucial step toward broader implementation in practical SHM deployments.

ACKNOWLEDGMENTS

This research is funded by dtec.bw -- Digitalization and Technology Research Center of the Bundeswehr. dtec.bw is funded by the European Union -- NextGenerationEU. We thank all DTEC Project supporters. For future research, both the experimental measurement data and the finite element model developed in this study are available upon request.

REFERENCES

[1] C. R. Farrar and K. Worden.” Structural Health Monitoring: A Machine Learning Perspective”. Chichester, UK: Wiley, 2012.

[2] U.S. Department of Defense.”Nondestructive Evaluation System Reliability Assessment, MIL-HDBK-1823A, 2009”.

[3] Y. Deng, X. Liu and L. Udpa, "Magneto-Optic Imaging for Aircraft Skins Inspection: A Probability of Detection Study of Simulated and Experimental Image Data," in IEEE Transactions on Reliability, vol. 61, no. 4, pp. 901-908, Dec. 2012, doi: 10.1109/TR.2012.2221613.

[4] Berens, Alan P. "NDE reliability data analysis." *ASM Handbook*. 17 (1989): 689-701.

[5] Kabban, Christine & Greenwell, Brandon & Desimio, Martin & Derriso, Mark. (2015). “The probability of detection for structural health monitoring systems: Repeated measures data. Structural Health Monitoring”. 14. 252-264. 10.1177/1475921714566530

[6] Meeker, W., Roach, D. & Kessler, Seth. (2019). “Statistical Methods for Probability of Detection in Structural Health Monitoring”. 10.12783/shm2019/32095.

[7] Knopp, J. Aldrin, John Lindgren, E. & Annis, Charles. (2007). “Investigation of a Model-Assisted Approach to Probability of Detection Evaluation (Preprint)”. AIP Conference Proceedings. 894. 1775-1782. 10.1063/1.2718178.

[8] Kevin Smith, Bruce Thompson, Bill Meeker, Tim Gray, Lisa Brasche; Model-Assisted Probability of Detection Validation for Immersion Ultrasonic Application. AIP Conf. Proc. 21 March 2007; 894 (1): 1816–1822. https://doi.org/10.1063/1.2718184

[9] Calmon, Pierre & Mesnil, Olivier & Miorelli, Roberto & Artusi, Xavier & CHAPUIS, BASTIEN & d'Almeida, Oscar. (2019). “Model Assisted Probability of Detection for Guided Wave Imaging Structural Health Monitoring”. 10.12783/shm2019/32190.

[10] G. E. Box and G. C. Tiao. “Bayesian Inference in Statistical Analysis”. New York: Wiley, 1992.

[11] D. Higdon, J. Gattiker, B. Williams, and M. Rightley. “Combining field data and computer simulations for calibration and prediction”. SIAM Journal on Scientific Computing, vol. 26, no. 2, pp. 448–466, 2004.

[12] Vogel, T., & Thöns, S. (2018). “Detection and localization of structural changes using Mahalanobis distance and frequency response functions”. *Structural Control and Health Monitoring*, 25(5), e2160. https://doi.org/10.1002/stc.2160.

[13] Bojana V. Rosić, Alexander Litvinenko, Oliver Pajonk, Hermann G. Matthies. (2012) “Sampling-free linear Bayesian update of polynomial chaos representations”. Journal of Computational Physics, Volume 231, Issue 17, 2012.

[14] Bojana V. Rosić, Anna Kučerová, Jan Sýkora, Oliver Pajonk, Alexander Litvinenko, Hermann G. Matthies. (2013). “Parameter identification in a probabilistic setting”. Engineering Structures, Volume 50, 2013.

[15] F. Marsili, A. Mendler, F. Landi, und S. Kessler. (2023). “Minimum detectable changes based on linear Bayesian filters”. *Mechanical Systems and Signal Processing*, Bd. 202, S. 110656, Nov. 2023, doi: 10.1016/j.ymssp.2023.110656.

[16] Chopra, A.K. (2012). “Dynamics of Structures: Theory and Applications to Earthquake Engineering (4th Edition)”. Pearson.

[17] Ewins, D.J. (2000). “*Modal Testing: Theory, Practice and Application* (2nd ed.)”. Research Studies Press.